Predictive Voltage Control of Four-Leg Converter

Jason Foster, Nan Duan, Lutong Ji, Yu Zhou, Mohammad Alrashidi, Venkata Yaramasu
(jf727, nd399, lj384, yz245, mta48, venkata.yaramasu) @nau.edu

***Abstract*— This paper explores predictive voltage control for a 2-level 4-leg converter. The proposed algorithm uses inverter currents, load current and load voltages as feedback. The proposed algorithm uses this feedback to predict the future load behavior of the load voltages. A cost function will select the optimal switching state based on the predicted and measured Feedbacks that have the minimal error. The proposed control scheme is validated by MATLAB Simulink results and in dSPACE DS1103 based experimental results with linear, unlinear, balanced and unbalanced loads.**

***Index terms*— digital control, model predictive control, voltage control, power electronics, renewable energy.**

I. INTRODUCTION

Standalone power systems are very popular to supply remote equipment and customs in many applications [1],[2], like the Navajo communities in Arizona. The standalone power systems are the alternative solution at locations which cannot access to the main power grid or require lots of economic costs and in the place where the use of electricity is necessary. For example, islands; telecommunication stations; satellite earth stations and the installation of service system for oil and gas pipelines [3]-[5]. The photovoltaic (PV), solar thermal, wind energy conversion system (WECS) generators, battery banks and diesel or biofuel generator have been extensively installed in such standalone power systems. The three-phase four-leg converters are widely used in many commercial and industrial applications, such as, the standalone (off-grid) operation, electric drives and dynamic voltage restorers that demand tight output voltage control with unbalanced and nonlinear loads [6]-[8]. In order to provide transformerless neutral connection and symmetrical sinusoidal voltage to the loads, the three-phase converter with an additional fourth (neutral) leg and output with the connection of inductor and capacitor (LC) filter is proved to the best candidate in standalone power systems [9]. The reason for using four-leg converter instead of three-leg converter is the four-leg converter provides 15-16% higher DC bus utilization compare to the three-leg converters. And it also provides lower ripple on the DC-link voltage, smaller size for dc-link capacitors, and the switching states increase from 8 to 16, the more switching states can provide greater control of converter [4].

For different output of four-leg converter such as voltage and current can be controlled depending on the different application. The current control is usually used in distributed generation with grid connection. The voltage control is used for standalone distributed generation [5]. A lot of control scheme techniques have been developed so far. There are a special control schemes for power converters, the classical voltage control techniques for a four-leg converter can use proportional-integral (PI) controllers including stationary ($\alpha\beta\gamma$), synchronous ($dq0$) and natural ($abcn$), pole placement regulators controllers and variable structure, sliding mode control to eliminate steady-state voltage error and a modulation stage to generate the gating signals. The modulation schemes for four-leg converters generally use carrier-based sinusoidal pulse-width modulation (SPWM) and 3-D space vector modulation (3D-SVM). The SPWM is based on the real-time implementation and the switching angle calculation that is complicated. Despite the 3D-SVM can provide lower switching frequency, high-rated DC-link utilization and minimum output distortion compare to the SPWM. However, 3D-SVM is still a complicated method in hardware and software implement, because of it requires large computational capacity for the 3D transformations [4]-[6],[10]-[14].

The finite control set model predictive control (FCS-MPC) that are usually used in power electronics and drives now. The advantage of FCS-MPC is the simple concept and fast dynamic response, and this scheme does not require internal current control loops and modulators which means this is a simple and very flexible control scheme that allows easy inclusion of the nonlinearities and constraints such as switching frequency minimization, spectrum shaping, common-mode voltage minimization and switching/conduction loss minimization that can be included in the design of controller [8],[9]. Similar with the carrierless modulation schemes, this method operates with the variable switching frequency, which means it can provide for complex modeling and higher computational capacity [11]. The predictive voltage control (PVC) with output LC filter are analyzed in literate for a four-leg converter [12].

In this paper, the object is improving the PVC for 4-leg converter with LC filter, the previous vision of PVC [13] had the drawbacks when the voltage got steady-state, there are ripple interference at the peak value of voltage. Paper will introduce the solution that solve the ripple problem at peak value and to reduce the percentage total harmonic distortion (%THD) to get appropriate load current. To validate the feasibility of the proposed control method the simulation is carried out using MATLAB/Simulink software, the experimental are presented using the dSPACE DS1103, and dSPACE control desk rapid prototyping real-time implementation.

This paper is organized as follows: in section II, the modeling of 4-leg converter strategy is presented, followed

by the modeling of predictive control of the 4-leg converter in section III. In section IV, simulation and experiment results are presented, and finally appropriate conclusions are drawn in section V.

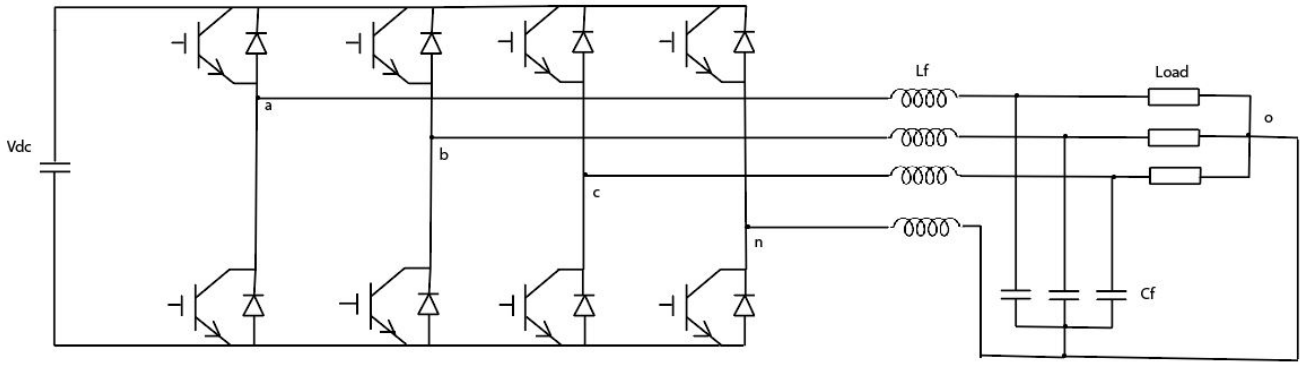

Fig. 1. Proposed converter schematic

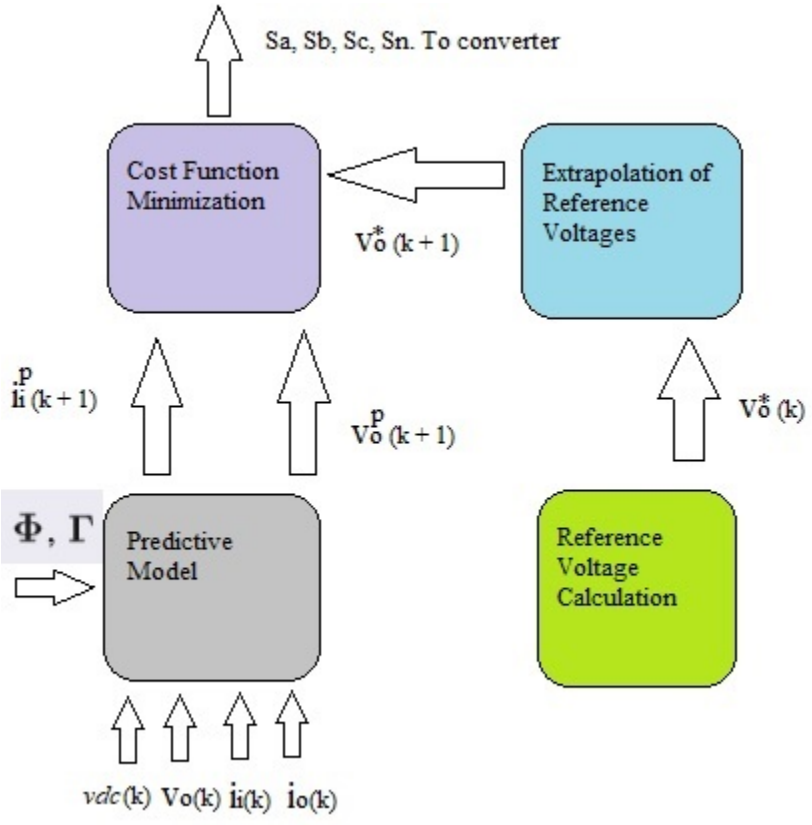

Fig. 2. Model predictive control block diagram

II. FOUR LEG INVERTER MODEL

Fig. 1 shows three-phase four-leg inverter with LC filter. Comparing to traditional three-phase inverter, four-leg inverter have a neutral point.

The neutral point is n. The inductors' current are i_{ia}, i_{ib}, i_{ic}. The load current are i_{oa}, i_{ob}, i_{oc}. The inverter voltage are v_{ia},v_{ib},v_{ic},v_{in}. The voltage between the capacitors are v_{oa}, v_{ob}, v_{oc}. The inductors value is L_i, and the resistance of inductors is r_i. The value of capacitors is C_o. The filter can be expressed by the differential equations as follows:

$$\begin{aligned} v_{ia} &= L_i \frac{di_{ia}}{dt} + v_{oa} \\ v_{ib} &= L_i \frac{di_{ib}}{dt} + v_{ob} \\ v_{ic} &= L_i \frac{di_{ic}}{dt} + v_{oc} \end{aligned} \tag{1}$$

$$\begin{aligned} i_{ia} &= C_o \frac{dv_{oa}}{dt} + i_{oa} \\ i_{ib} &= C_o \frac{dv_{ob}}{dt} + i_{ob} \\ i_{ia} &= C_o \frac{dv_{oc}}{dt} + i_{oc} \end{aligned} \tag{2}$$

Based on (1), the inverter current can be expressed as:

$$\frac{d}{dt}\begin{bmatrix} i_{ia} \\ i_{ib} \\ i_{ic} \end{bmatrix} = -\frac{1}{L_i}\begin{bmatrix} v_{oa} \\ v_{ob} \\ v_{oc} \end{bmatrix} + \frac{1}{L_i}\begin{bmatrix} v_{ia} \\ v_{ib} \\ v_{ic} \end{bmatrix} \tag{3}$$

As such, (2) can be expressed as follows:

$$\frac{d}{dt}\begin{bmatrix} v_{oa} \\ v_{ob} \\ v_{oc} \end{bmatrix} = \frac{1}{C_o}\begin{bmatrix} i_{ia} \\ i_{ib} \\ i_{ic} \end{bmatrix} + -\frac{1}{C_o}\begin{bmatrix} i_{oa} \\ i_{ob} \\ i_{oc} \end{bmatrix} \tag{4}$$

From (4) it is known that there are three independent variables in v_{ia}, v_{ib}, v_{ic}, v_{in} controlling the system output voltage. So a change in one of them will affect the output voltage value. If changing one of v_{ia}, v_{ib}, v_{ic}, the balance of system will be broken. But if finding a relationship between v_{ia}, v_{ib}, v_{ic} and v_{in}, the system will be balanced.

Based on (1), (2), (3) and (4), the analysis result is as follow:

$$v_{\mathbf{i,abc}} = r_i * i_{\mathbf{i,abc}} + L_i * \frac{di_{\mathbf{i,abc}}}{dt} + v_{\mathbf{o,abc}} \tag{5}$$

III. PREDICTIVE VOLTAGE CONTROL SCHEME

The proposed MPC scheme used is modeled below in figure 2. By implementing the model in figure 2 within MATLAB the $(k+1)$ voltage vectors can be computed for cost-function analysis. By iterating through all 16 values of V_o and the stationary frame load voltages a cost function is used to determine which vectors will provide the most optimal switching state for the next instance in time, $(k+1)$.

After predicting the inverter voltage the output voltage vector is generated. Once generated it then goes through the cost function shown below:

$$g = (v^*_{o\alpha} - v_{o\alpha}(k+1)^p)^2 + (v^*_{o\beta} - v_{o\beta}(k+1)^p)^2 + (v^*_{o\gamma} - v_{o\gamma}(k+1)^p)^2 \tag{6}$$

Where $v^*_{o\alpha}$, $v^*_{o\beta}$ and $v^*_{o\gamma}$ are reference output voltages and $v_{o\alpha}(k+1)^p$, $v_{o\beta}(k+1)^p$, and $v_{o\gamma}(k+1)^p$ are the predicted output voltages. After 16 iterations the algorithm will decide which switching state will create the lowest g and apply that to the converter for the next switching state and begin the process again.

In order to predict the output voltage vectors a discrete-time model of the converter must be developed. Once the discrete-time model is created the output voltages and currents are transformed to $\alpha\beta\gamma$ space. The transformation to $\alpha\beta\gamma$ space is described below:

$$\begin{bmatrix} S_\alpha \\ S_\beta \\ S_\gamma \end{bmatrix} = 2/3 * \begin{bmatrix} 1 & -1/2 & -1/2 \\ 0 & \sqrt{3}/2 & -\sqrt{3}/2 \\ 1/2 & 1/2 & 1/2 \end{bmatrix} * \begin{bmatrix} S_a - S_n \\ S_b - S_n \\ S_c - S_n \end{bmatrix} \tag{7}$$

Where S denotes whether the switch is open, 1, or closed, 0.

Once the three phase (a, b, c) voltage and currents are transformed into (α, β, γ) space the discrete-time equations utilized to determine the value of the (k+1) voltage and current vectors are seen below:

$$V_i(k+1) = V_{dc} * S_i \tag{8}$$

$$\begin{bmatrix} v_o(k+1) \\ i_i(k+1) \end{bmatrix} = \phi * \begin{bmatrix} V_o(k) \\ I_i(k) \end{bmatrix} + \Gamma * \begin{bmatrix} v_i(k+1) \\ i_o \end{bmatrix} \tag{9}$$

where θ and Γ are 6 by 6 matrices described as,

$$\phi = e^{A_{ct}} * T_s \tag{10}$$

$$\Gamma = A_{ct}^{-1}\left[\theta\right] - \left[ID_{6x6}\right] * \left[B_{ct}\right] \tag{11}$$

and A_{ct} and B_{ct} are described as,

$$A_{ct} = \begin{bmatrix} 0_{3x3} & \frac{I_{3x3}}{C_f} \\ -L_{eq}^{-1} & -L_{eq}^{-1} * R_{eq} \end{bmatrix} \tag{12}$$

$$B_{ct} = \begin{bmatrix} 0_{3x3} & \frac{-I_{3x3}}{C_f} \\ L_{eq}^{-1} & 0_{3x3} \end{bmatrix} \tag{13}$$

with L_{eq} and R_{eq} described as,

$$L_{eq} = \begin{bmatrix} L_f + L_n & L_n & L_n \\ L_n & L_f + L_n & L_n \\ L_n & L_n & L_f + L_n \end{bmatrix} \tag{14}$$

$$R_{eq} = \begin{bmatrix} R_f + R_n & R_n & R_n \\ R_n & R_f + R_n & R_n \\ R_n & R_n & R_f + R_n \end{bmatrix} \tag{15}$$

Where I_{3x3} and 0_{3x3} is the 3 by 3 identity and zero matrix, respectively. T_s is the sampling interval, 50μs.

IV. EXPERIMENTAL RESULTS

To validate the effectiveness of the proposed control scheme, the experimental results are captured under the conditions of steady state and transient state, with balanced, unbalanced, and nonlinear loads. All the cases will also be tested in conventional methods: Dr. Yaramasu 2012 and classical PWM. Case 1 tests with balanced references and balanced loads, case 2 tests with balanced references and unbalanced plus Nonlinear Load (NL), case 3 tests with unbalanced references and balanced loads and case 4 tests with unbalanced references and unbalanced plus NL.

A. Steady-State Analysis

TABLE I
VALUES FOR TEST CASES

Case 1	Case 2	Case 3	Case 4
V_{oa}^* = 120V	V_{oa}^* = 120V	V_{oa}^* = 120V	V_{oa}^* = 120V
V_{ob}^* = 120V	V_{ob}^* = 120V	V_{ob}^* = 100V	V_{ob}^* = 100V
V_{oc}^* = 120V	V_{oc}^* = 120V	V_{oc}^* = 80V	V_{oc}^* = 80V
f_a^* = 60Hz	f_a^* = 60Hz	f_a^* = 60Hz	f_a^* = 60Hz
f_b^* = 60Hz	f_b^* = 60Hz	f_b^* = 60Hz	f_b^* = 60Hz
f_c^* = 60Hz	f_c^* = 60Hz	f_c^* = 60Hz	f_c^* = 60Hz
R_a = 10Ω	R_a = 10Ω	R_a = 10Ω	R_a = 10Ω
R_b = 10Ω	R_b = 11Ω	R_b = 10Ω	R_b = 11Ω
R_c = 10Ω	$R_c = 5\Omega + NL$	R_c = 10Ω	$R_c = 5\Omega + NL$

The experimental results for case A are presented in Fig.TBD. Due to the balanced reference and balanced load, a current of $10A_{rms}$ at 60Hz circulates through phase a, b, c in three methods are shown in Fig. TBD. The load voltages to their respective references have a good tracking of their respective references are observed in Fig. TBD. The experimental results with balanced references and unbalanced nonlinear load are shown in Fig. TBD. In this test, balanced references and unbalanced nonlinear load are considered in all three methods. As shown in Fig. TBD, the load voltage remains sinusoidal. Load current of i_{oa} = TBD A_{rms}, i_{ob} = TBD A_{rms}, i_{oc} = TBD A_{rms}, as shown in Fig. TBD. In this case, the controller maintains the voltage at reference value irrespective of the load. Unbalanced references and balanced load is presented in Fig. TBD. As shown in Fig. TBD, the load voltage remains sinusoidal with load current of of i_{oa} = TBD A_{rms}, i_{ob} = TBD A_{rms}, i_{oc} = TBD A_{rms}, as shown in Fig. TBD. The experimental results with unbalanced references and unbalanced nonlinear load are shown in Fig. TBD. Because of unbalanced nonlinear load conditions, a neutral current circulates through the fourth leg as depicted in Fig. TBD, but the load voltages remain sinusoidal with a very good tracking to their respective references as shown in Fig. TBD. Comparing the three methods in four cases as shown in table 1, the proposed predictive voltage control has a better tracking of load voltages to their respective references, especially in higher voltage. The proposed method reduced the ripples in peak voltage value.

B. Transient Analysis

TABLE II
VALUES FOR TEST CASES

Case 1	Case 2	Case 3	Case 4
V_{oa}^* = 0-120V	V_{oa}^* = 0-120V	V_{oa}^* = 0-120V	V_{oa}^* = 0-120V
V_{ob}^* = 0-120V	V_{ob}^* = 0-120V	V_{ob}^* = 0-100V	V_{ob}^* = 0-100V
V_{oc}^* = 0-120V	V_{oc}^* = 0-120V	V_{oc}^* = 0-80V	V_{oc}^* = 0-80V
f_a^* = 0-120Hz	f_a^* = 0-120Hz	f_a^* = 0-120Hz	f_a^* = 0-120Hz
f_b^* = 0-120Hz	f_b^* = 0-120Hz	f_b^* = 0-120Hz	f_b^* = 0-120Hz
f_c^* = 0-120Hz	f_c^* = 0-120Hz	f_c^* = 0-120Hz	f_c^* = 0-120Hz
R_a = 10Ω	R_a = 10Ω	R_a = 10Ω	R_a = 10Ω
R_b = 10Ω	R_b = 11Ω	R_b = 10Ω	R_b = 11Ω
R_c = 10Ω	$R_c = 5\Omega + NL$	R_c = 10Ω	$R_c = 5\Omega + NL$

Increasing the frequency from 60Hz to 120Hz causes a step change in all the five different cases. Although there is a fast step change, the results show a fast-dynamic response. The step change duration is approximately in microseconds. The current flows through the fourth leg due to probably not having PI controllers. Results shows four different cases during a 50 μs time. Case D has the least total harmonic distortion percentage compared to the other three cases. Comparing the simulation and experimental results, Case A, B, and C have close results as expected in the experimental results.

C. Quantitative Analysis

In this section, the reduction of the neutral-leg switching frequency is verified. The references and loads are balanced (case A). The load voltages to their respectively references(v_o^*), average switching frequency (f_{sw}), reference tracking error (%evo), and %THD are presented through experimental tests in Figs. 11 and 12, respectively. As shown in Figs. 11and 12, with V_o^* increase, f_{sw} decrease. Reference tracking error (%evo) increases with %THD increases.

- Relationship between frequency and the reference output voltage

TABLE III

plot goes here

- Relationship between Vo THD and reference tracking error (%evo)

TABLE IV

plot goes here

D. V_o Estimation

The objective of this section is to show how voltage experimentally of proposed method and conventional methods track the referenced voltage. Fig. 6 presents the output and reference voltages in alpha-beta plane.

TABLE V

CASE 5: UNBALANCED REFERENCES AND UNBALANCED + NONLINEAR LOAD

SPC 2018 X-Y plot	Yaramasu 2012 X-Y plot	Classical X-Y plot

The output voltage reference of proposed method is accurately tracked as shown in Fig. These results conclude that the proposed predictive voltage control is able to control the output better compared to the conventional methods.

After a three phase four leg converters was developed in the lab. The experiment was performed in steady state with unbalanced, balanced and nonlinear loads. [Results TBD]

As mentioned above, there are three phase currents, I(a),I(b) and I(c). The power supply provides a voltage of $350v$, the output load resistance of 10Ω and output voltage frequency of 60Hz. The capacitor filter as well as the inductor filter would be C_f = 60μF and L_f = 2.5 mH. Moreover, there is a neutral resistor of 0.022Ω. Additionally, a DC link resistance and a DC link capacitance of 1Ω and 2000μF. Those values were used in the simulation before actually being tested in the lab. After preforming the experiment, the values turned out to be similar to the simulation values initially obtained.

V. CONCLUSION

FCS-MPC with a voltage control method has been proposed in this paper to control the three-phase four-leg converter with an output LC filter. The control algorithm tests each of the 16 possible switching states and then chooses optimal switching state that minimizes the cost function. The ideal minimum of the cost function is zero and represents the perfect regulation of the output voltages with the balancing of the capacitor voltages. With the predictive control, the control of load voltage with less error has been achieved under the balanced, un-balanced and nonlinear load conditions, and the load voltages are tracked with acceptable error compare to the reference. It is possible to get less ripple peak voltage in the process of steady-state when getting the appropriate predictive modulation.

ACKNOWLEDGMENT

This work is completed as a part of Undergraduate Capstone Design Project. The authors wish to thank the financial support from the School of Informatics, Computing, and Cyber Systems (SICCS), and the College of Engineering, Forestry, and Natural Sciences (CEFNS), Northern Arizona University.

References are important to the reader; therefore, each citation must be complete and correct. If at all possible, references should be commonly available publications.

REFERENCES

[1] E. Ribeiro, A. J. M. Cardoso and C. Boccaletti, "Power conditioning supercapacitors in combination with batteries for stand-alone power systems," International Symposium on Power Electronics Power Electronics, Electrical Drives, Automation and Motion, Sorrento, 2012, pp. 914-919.

[2] V. Yaramasu, M. Rivera, M. Narimani, B. Wu and J. Rodriguez, "Model Predictive Approach for a Simple and Effective Load Voltage Control of Four-Leg Inverter With an Output LC Filter," in IEEE Transactions on Industrial Electronics, vol. 61, no. 10, pp. 5259-5270, Oct. 2014.

[3] N. Sa-ngawong and I. Ngamroo, "PSO-based Sugeno fuzzy logic controller of photovoltaic generator for frequency stabilization in stand-alone power system," 2013 IEEE PES Asia-Pacific Power and Energy Engineering Conference (APPEEC), Kowloon, 2013, pp. 1-6.

[4] S. V. Brovanov, T. E. Shults and A. V. Sidorov, "Stand-alone power supply system using photovoltaic panels and diode-clamped multilevel inverter," 2014 15th International Conference of Young Specialists on Micro/Nanotechnologies and Electron Devices (EDM), Novosibirsk, 2014, pp. 464-467.

[5] V. Yaramasu, B. Wu, M. Rivera, J. Rodriguez and A. Wilson, "Cost-function based predictive voltage control of two-level four-leg inverters using two step prediction horizon for standalone power systems," 2012 Twenty-Seventh Annual IEEE Applied Power Electronics Conference and Exposition (APEC), Orlando, FL, 2012, pp. 128-135.

[6] V. Yaramasu, J. Rodriguez, B. Wu, M. Rivera, A. Wilson and C. Rojas, "A simple and effective solution for superior performance in two-level four-leg voltage source inverters: Predictive voltage control," 2010 IEEE International Symposium on Industrial Electronics, Bari, 2010, pp. 3127-3132.

[7] M. Alhasheem, T. Dragicevic and F. Blaabjerg, "Evaluation of multi predictive controllers for a two-level three-phase stand-alone voltage source converter," 2017 IEEE Southern Power Electronics Conference (SPEC), Puerto Varas, 2017, pp. 1-6.

[8] V. Yaramasu, M. Rivera, B. Wu and J. Rodriguez, "Predictive control of four-leg power converters," 2015 IEEE International Symposium on Predictive Control of Electrical Drives and Power Electronics (PRECEDE), Valparaiso, 2015, pp. 121-125.

[9] V. Yaramasu, B. Wu, M. Rivera and J. Rodriguez, "Enhanced model predictive voltage control of four-leg inverters with switching frequency reduction for standalone power systems," 2012 15th International Power Electronics and Motion Control Conference (EPE/PEMC), Novi Sad, 2012, pp. DS2c.6-1-DS2c.6-5.

[10] S. Bayhan, M. Trabelsi and H. Abu-Rub, "Model Predictive Control of Z-Source four-leg inverter for standalone Photovoltaic system with unbalanced load," 2016 IEEE Applied Power Electronics Conference and Exposition (APEC), Long Beach, CA, 2016, pp. 3663-3668.

[11] T. Dragicevic, M. Alhasheem, M. Lu and F. Blaabjerg, "Improved model predictive control for high voltage quality in microgrid applications," 2017 IEEE Energy Conversion Congress and Exposition (ECCE), Cincinnati, OH, 2017, pp. 4475-4480.

[12] C. Leffler et al., "Guidelines for dSPACE-based real-time implementation of predictive current control for grid-connected converters," 2017 IEEE Southern Power Electronics Conference (SPEC), Puerto Varas, 2017, pp. 1-8.

[13] C. F. Garcia, M. E. Rivera, J. R. Rodrguez, P. W. Wheeler and R. S. Pea, "Predictive Current Control With Instantaneous Reactive Power Minimization for a Four-Leg Indirect Matrix Converter," in IEEE Transactions on Industrial Electronics, vol. 64, no. 2, pp. 922-929, Feb. 2017.

[14] K. Antoniewicz, M. Jasinski, M. P. Kazmierkowski and M. Malinowski, "Experimental research on model predictive control of 3-level 4-leg Flying Capacitor Converter operating as Shunt Active Power Filter," IECON 2015 - 41st Annual Conference of the IEEE Industrial Electronics Society, Yokohama, 2015, pp. 000036-000041.